Supplemental Document

Optics Letters

In situ characterization of few-femtosecond laser pulses by learning from first-principles calculations: supplement

Otfried Geffert,[1,*] Daria Kolbasova,[1,2] Andrea Trabattoni,[1,3] Francesca Calegari,[1,4] and Robin Santra[1,2]

[1]*Center for Free-Electron Laser Science CFEL, Deutsches Elektronen-Synchrotron DESY, Notkestr. 85, 22607 Hamburg, Germany*
[2]*Department of Physics, Universität Hamburg, Notkestrasse 9-11, 22607 Hamburg, Germany*
[3]*Institute of Quantum Optics, Leibniz University Hannover, Welfengarten 1, 30167 Hannover, Germany*
[4]*Department of Physics, Universität Hamburg, Luruper Chaussee 149, 22761 Hamburg, Germany*
[*]*Corresponding author:* *otfried.geffert@desy.de*

This supplement published with Optica Publishing Group on 3 August 2022 by The Authors under the terms of the Creative Commons Attribution 4.0 License in the format provided by the authors and unedited. Further distribution of this work must maintain attribution to the author(s) and the published article's title, journal citation, and DOI.

Supplement DOI: https://doi.org/10.6084/m9.figshare.20089604

Parent Article DOI: https://doi.org/10.1364/OL.460513

1. STRONG-FIELD IONIZATION OF ARGON USING TDCIS

TDCIS [1, 2] is an ab-initio electronic-structure technique, in which the time-dependent wave function is restricted, with respect to the full N-body wave function, to spin-singlet conserving single-particle excitations from the Hartree-Fock (HF) ground-state determinant. The N-electron wave function ansatz for TDCIS reads

$$|\Psi(t)\rangle = \alpha_0(t)|\Phi_0\rangle + \sum_{a,i} \alpha_i^a(t)|\Phi_i^a\rangle, \tag{S1}$$

where $|\Phi_0\rangle$ is the HF ground state, and the $|\Phi_i^a\rangle = c_a^\dagger c_i|\Phi_0\rangle$ are one-particle–one-hole (1p-1h) excitations, where an electron from orbital i is promoted to orbital a. The time-dependent Schrödinger equation reads

$$i\frac{\partial}{\partial t}|\Psi,t\rangle = \left[\hat{H}_0 + \hat{H}_1 - E_{HF} + \hat{\vec{p}}\cdot\vec{A}(t)\right]|\Psi,t\rangle. \tag{S2}$$

Here, $\hat{H}_0$ is the mean-field Hamiltonian associated with the HF ground state, $\hat{H}_1$ is the residual electron-electron interaction (i.e., the electron-electron interaction minus the HF mean-field potential), E_{HF} is the HF ground-state energy, and $\hat{\vec{p}}\cdot\vec{A}(t)$ is the light-matter interaction within the velocity form (electric-dipole approximation), where $\vec{A}(t)$ is the vector potential and $\hat{\vec{p}}$ is the electron canonical momentum.

The ground electronic configuration for Ar is [Ne]$3s^2 3p^6$. We take into account spin-orbit coupling, as described in [3], and use the experimentally known electron binding energies [4]. In our calculations, we only allow the $3p$ and $3s$ orbitals to be active, whereas all other orbitals are frozen (not affected by the laser field). The laser field amplitude in our calculations is $E = 0.015$ a.u. ($I \approx 7.88\,\mathrm{TW/cm^2}$) and its frequency $\omega = 0.061$ a.u. ($\nu \approx 420$ THz). In order to perform a precise and stable calculation, we placed the edge of the numerical grid at $r_{\max} = 80$ a.u. with respect to the atomic nucleus at $r = 0$ and used a grid size of $N = 300$ grid points.

When the wave packet reaches the end of the numerical grid, artificial reflections arise, which lead to unphysical results. We suppressed them by applying a complex absorbing potential (CAP) [5–10] near the end of the grid. Thus,

$$\hat{H}_0 = \hat{F} - i\zeta\hat{W} \tag{S3}$$

is the sum of the HF ground-state Fock operator $\hat{F}$ and a CAP defined by

$$W(r) = \theta(r - r_{abs})(r - r_{abs})^2, \tag{S4}$$

where $\theta(r)$ is the Heaviside step function, and r is the distance from the nucleus. This CAP vanishes below $r = r_{\mathrm{abs}}$, after which it is a quadratically growing potential. The CAP strength ζ has to be chosen carefully to avoid reflections from the grid wall at $r = r_{\max}$ or from the CAP itself [5, 10]. In our calculations, $\zeta = 0.5$ and $r_{\mathrm{abs}} = 50$ a.u. The maximum electronic angular-momentum allowed in our calculations is $l_{\max} = 10$. Orbitals with HF energies higher than 20 a.u. (real part of the orbital energies) were determined not to contribute significantly and have been omitted from the electronic wave-packet propagation calculations.

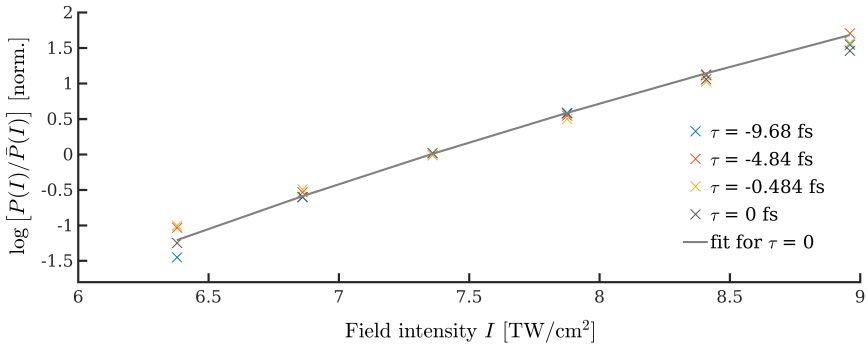

Fig. S1. Dependence of the ion yield on the field intensity I, in a range of intensities satisfying Eq. (S5). The illustration is given for different delays τ, zero GDD, $\chi_t = 400$ a.u., and zero relative phase shift $\Delta\phi$. The power law determined for $\tau = 0$ (solid line) satisfactorily describes the trend for all values of τ.

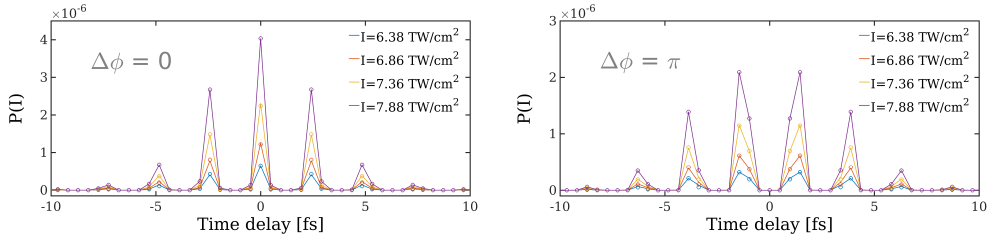

Fig. S2. Demonstration of the insensitivity, to τ and $\Delta\phi$, of the exponent n in Eq. (S5) (for zero GDD and $\chi_t = 400$ a.u.). Using the n obtained for $\tau = 0$ and $\Delta\phi = 0$, together with the $C(\tau, \Delta\phi)$ determined for a reference intensity, autocorrelation patterns at other intensities can be reliably predicted through Eq. (S5). The predictions (solid lines) are compared with the TDCIS calculations (dots of the same color).

2. INTENSITY DEPENDENCE OF THE AUTOCORRELATION PATTERNS

In an experiment, the beam intensity profile is not uniform in space. Thus, atoms in a gas target can get ionized in spatial regions that differ from each other with respect to intensity. In the following, we demonstrate that the autocorrelation patterns of interest are expected to be insensitive to the resulting volume integration (or volume averaging) effects. To this end, we performed TDCIS calculations for a range of intensities at different delays. Exemplary results are presented in Fig. S1, together with the fit to a power law,

$$P(I) = CI^n, \tag{S5}$$

for $\tau = 0$.

Figure S1 illustrates that $P(I)$ fits Eq. (S5) with $n = 8.679$ in the range of intensities $I < 8\,\mathrm{TW/cm^2}$, and for different time delays τ. The binding energy for the outer-valence shell of Ar is $E_b \approx 15.7$–15.9 eV. Hence, ionization requires the absorption of at least 9–10 photons ($\omega = 1.65$ eV). However, as the short

pulses provide a broad photon energy spectrum, the ionization may on occasion require a smaller number of photons, which is compatible with an n a bit below 9 in Eq. (S5).

More importantly, Fig. S1 shows that the exponent, n, in Eq. (S5) is relatively insensitive to the delay τ. This means that, for a given set of pulse parameters, the delay dependence of the autocorrelation patterns is captured almost exclusively by the parameter C in Eq. (S5). As demonstrated in Fig. S2, the structure of the autocorrelation patterns does not change much for the aforementioned range of intensities: They differ from each other only through a τ-independent multiplicative factor. We have verified that this conclusion remains valid for other pulse-parameter values. Therefore, we expect that for beam peak intensities below $8\,\mathrm{TW/cm^2}$, volume integration does not affect the shape of the autocorrelation patterns of interest here. The characterization of pulses with an intensity outside the range $1 - 8\ \mathrm{TW/\ cm^2}$ requires an extension of the current database. Characterization of lower-intensity pulses may require a change of the target sample to an atomic species with a lower ionization threshold.

REFERENCES

1. L. Greenman, P. J. Ho, S. Pabst, E. Kamarchik, D. A. Mazziotti, and R. Santra, "Implementation of the time-dependent configuration-interaction singles method for atomic strong-field processes," Phys. Rev. A **82**, 023406 (2010).
2. N. Rohringer, A. Gordon, and R. Santra, "Configuration-interaction-based time-dependent orbital approach for ab initio treatment of electronic dynamics in a strong optical laser field," Phys. Rev. A **74**, 043420 (2006).
3. S. Pabst, A. Sytcheva, A. Moulet, A. Wirth, E. Goulielmakis, and R. Santra, "Theory of attosecond transient-absorption spectroscopy of krypton for overlapping pump and probe pulses," Phys. Rev. A **86**, 063411 (2012).
4. A. C. Thompson, D. T. Attwood, E. M. Gullikson, M. R. Howells, J. B. Kortright, A. L. Robinson, J. H. Underwood, K.-Je Kim, J. Kirz, I. Lindau, P. Pianetta, H. Winick, G. P. Williams, J. H. Scofield, and D. Vaughan, "X-ray data booklet," https://xdb.lbl.gov/.
5. A. Goldberg and B. W. Shore, "Modelling laser ionisation," J. Phys. B: At. Mol. Opt. Phys. **11**, 3339–3347 (1978).
6. C. Leforestier and R. E. Wyatt, "Optical potential for laser induced dissociation," J. Chem. Phys. **78**, 2334–2344 (1983).
7. G. Jolicard and E. J. Austin, "Optical potential stabilisation method for predicting resonance levels," Chem. Phys. Lett. **121**, 106–110 (1985).
8. U. V. Riss and H. D. Meyer, "Calculation of resonance energies and widths using the complex absorbing potential method," J. Phys. B: At. Mol. Opt. Phys. **26**, 4503–4535 (1993).
9. R. Santra and L. S. Cederbaum, "Non-hermitian electronic theory and applications to clusters," Phys. Rep. **368**, 1–117 (2002).
10. J. Muga, J. Palao, B. Navarro, and I. Egusquiza, "Complex absorbing potentials," Phys. Rep. **395**, 357–426 (2004).